ISBN: 978-3-95450-214-1 ISSN: 2673-5490 doi:10.18429/JACoW-IPAC2021-TUPAB362

PHYSICAL DESIGN OF ELECTROSTATIC DEFLECTOR IN CSNS MUON SOURCE

Y. W. Wu †, J. Y. Tang, C. D. Deng, Y. Hong, X. Wu, S. Li, Y. Q. Liu
Spallation Neutron Source Science Center (SNSSC), Dongguan, China

Abstract

CSNS will build a muon source at the end of the RTBT. In the current design, the muon source proposes two schemes, namely the baseline scheme and the baby scheme. High voltage electrostatic deflectors (ESD) are used to deflect the beam in the two schemes. A three-channel ESD with 400 kV HV is employed in the baseline scheme and a 210 kV dual-channel ESD in the simplified scheme.

According to physical requirements, the electric field concentration factor is introduced, and the electrode of ESD is theoretically designed 2D and 3D simulations are carried out to analyze the characteristics of electric field distribution by OPERA. The geometry of the electrodes also met the requirements of electric field uniformity, high voltage resistance and mechanical strength at the same time. In the baseline scheme and the baby scheme, the ESD electric field concentration factors are 1.36 and 1.53, and the maximum electric field is 6.78 MV/m and 4.6 MV/m, respectively. The design meets the requirements and is reasonably feasible.

PHYSICAL CONSIDERATIONS

The layout of CSNS and muon source is shown in Fig. 1. For μSR experiments, positrons are the main contaminations, and should be controlled below 5% on the sample. General eliminating methods include degraders followed by a dipole, or Wien Filters composed of cross electromagnetic fields. Today's muon sources prefer to use the latter due to the emittance increasement caused by the degrader. Because of the thick target of EMuS, the beam emittance in the beamlines is quite large and it's difficult to focus onto a small sample required by typical μSR experiments. Even we can achieve this by collimation, however, the beam loss is much more than we expect. In addition, the direct application of Wien Filter to this beam with so large emittance results in extremely high requirements for a single Wien Filter, which will either increase the cost or bring more burden to operation and maintenance. As the repetition rate of CSNS proton accelerator is low, intensity is too high for the spectrometer if only one end-station is in use. So multiple end-stations are necessary.

In view of characteristics above, we adopt a spatial splitting method based on arc-shaped electrostatic separators on EMuS, which not only removes positrons, but also allows simultaneous beam supply for multiple end-stations. After the electrostatic separator, a septum magnet is placed to further deflect beam to ensure sufficient space for layout. Since the phase space of muons and positrons in the septum magnet will be partially remixed, we must ensure that the phase spaces of muons and positrons at the exit of the electrostatic separator are separated enough.

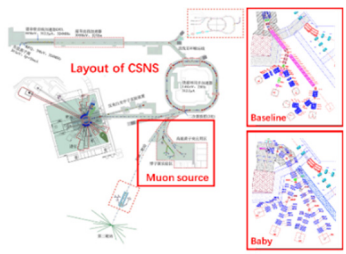

Figure 1: The layout of CSNS and muon source.

For the baby scheme, limited by the layout, we plan to use a dual-channel electrostatic separator, with one channel straight and field-free, and the other channel located in a field area produced by arc-shaped electrodes. For the baseline scheme, we plan to design a three-channel electrostatic separator, with symmetrical arc-shaped electrodes on both sides, and a narrow field-free straight-through channel in the middle. The effective length of the deflection channels is constrained to 0.6-0.7 meter to guarantee the transmission rate. Also, the deflection angle is approximately 10-20 degrees so that polarization won't be degraded too much. Follow the Eq. (1) below:

$$L = \rho\theta, E = vB, B\rho = \frac{p}{e} , \quad (1)$$

we can estimate that the strength of electric field is around a few MV/m, and the specific value is given by g4beamline simulation. In the baby scheme, positrons are about 14 times more than muons. The effective length of the separator is set to 0.66 m. When the deflection angle reaches 15.6 degrees, phase spaces of muons and the positrons are separated well enough, as shown in Fig. 2. The total voltage is 210 kV.

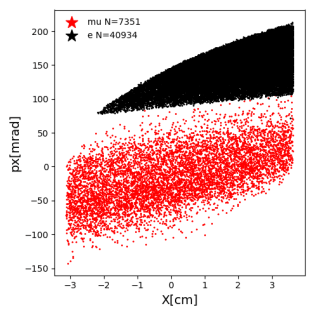

Figure 2: Phase spaces of muons and the positrons are separated by ESD in baby scheme.

As for the baseline scheme, superconducting solenoids collects positrons about 60 times of muons. With 0.7 m long separator, and 25 degrees deflection angle, phase spaces can be effectively separated. But now the voltage

† wuyw@ihep.ac.cn

ISBN: 978-3-95450-214-1 ISSN: 2673-5490 doi:10.18429/JACoW-IPAC2021-TUPAB362

has reached 400 kV. Electrodes with such high voltage will bring huge challenge for operations.

Considering the above, the technical parameters of ESD are shown in Table 1.

Table 1: The Technical Parameters of ESD

Scheme	Baseline	Baby
quantity	1	1
deflection angle (deg)	25	15.6
field area gap (mm)	80	50
field-free gap/entrance (mm)	24	140
field-free gap/exit (mm)	322	
electric field strength (MV/m)	5	3
voltage (kV)	400	210
effective length(m)	0.7	0.66
electrode width (mm)	300	200
power source	1	1

ELECTRODE DESIGN

In order to prevent high voltage local breakdown of the electrode, it is necessary to optimize the electrode [1, 2]. The electric field concentration factor β is introduced, which is defined as the ratio of the maximum field strength to the field strength in the central area, shown in Eq. (2). Empirically, it is required that $\beta < 2$, and the smaller β, the better the stability of the electric field between electrodes.

$$\beta = \frac{E_{max}}{E_0} \quad (2)$$

The maximum field intensity is concentrated at the end of the electrode. The larger the chamfer radius R, the smaller the maximum electric field intensity and the smaller the electric field concentration factor.

The cross section at the entrance of three-channel ESD for baseline scheme is shown in Fig. 3. It is shown R_1: 25 mm, R_2: 12.5 mm, R_3: 6.25 mm, R_4: 6.25 mm, L: 300 mm, d: 80 mm, a: 0.1 mm, b: 24 mm.

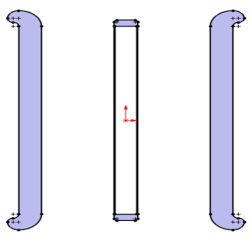

Figure 3: The cross section at the entrance of three-channel ESD.

ELECTRIC FIELD SIMULATION

ESD for Baseline Scheme

A three-channel electrostatic separator is adopted in baseline scheme. OPERA was used to perform 2D simulation of ESD, where R = 25 mm, electric field gap = 80 mm, electrode voltage 400 kV, and electrode length 300 mm. The simulation results show that the central electric field is 5 MV/m, the maximum electric field is 7.03 MV/m, and $\beta = 1.406$. The 2D electric field line distribution, the electric field intensity cloud diagram of the electrode and the vertical electric field distribution are shown in Figs. 4 and 5, respectively.

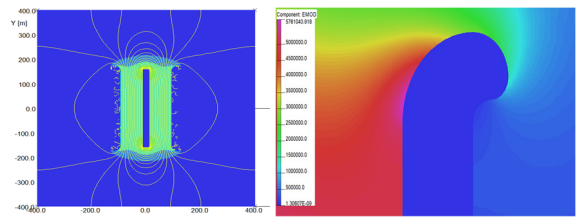

Figure 4: The 2D electric field line distribution and the electric field intensity cloud diagram of the electrode.

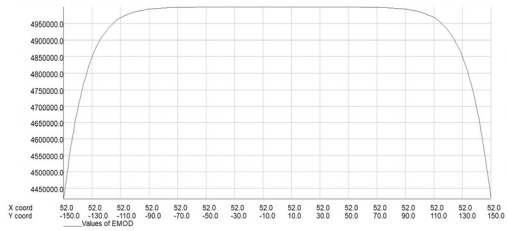

Figure 5: Vertical electric field distribution

On the basis of the 2D simulation results, a 3D simulation was performed, in which the entrance gap of the field-free zone was 24 mm, and the electric field gap was 80 mm. According to the simulation results, the maximum field strength at the electrode is 6.78 MV, which corresponds to $\beta = 1.36$. The 3D structure, the electric field line distribution diagram of the center section of the magnet, the electric field intensity cloud diagram, and the beam trajectory electric field distribution diagram are shown in Figs. 6, 7, and 8, respectively.

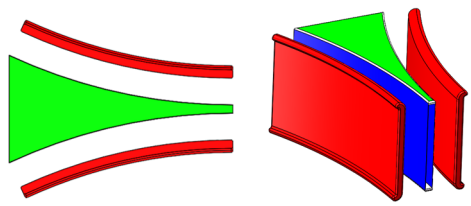

Figure 6: 3D structure.

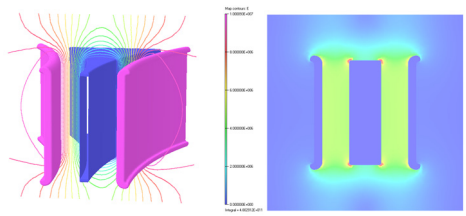

Figure 7: The electric field line distribution diagram of the center section of the magnet and the electric field intensity distribution cloud diagram.

ISBN: 978-3-95450-214-1 ISSN: 2673-5490 doi:10.18429/JACoW-IPAC2021-TUPAB362

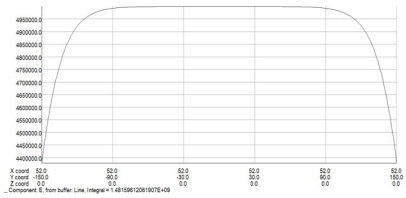

Figure 8: Electric field distribution along the beam trajectory.

ESD for Baby Scheme

The baby scheme adopts dual-channel ESD. Similar to the design of the baseline scheme, ESD is simulated in 2D by opera, where R1 = 25 mm, electric field gap = 70 mm, electrode voltage 210 kV, and electrode length 200 mm. The simulation result is that the central electric field is 3 MV/m, the maximum electric field is 3.92 MV/m, and the electric field concentration factor β = 1.31. The 2D size structure diagram, 2D electric field line distribution as shown in Fig. 9. The 2D electric field line distribution and the electric field intensity cloud diagram of the electrode are shown in Fig. 10. The vertical electric field distribution is shown in Fig. 11.

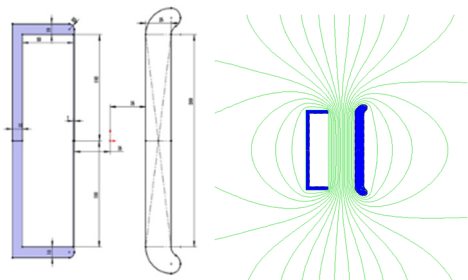

Figure 9: The 2D size structure diagram, 2D electric field line distribution.

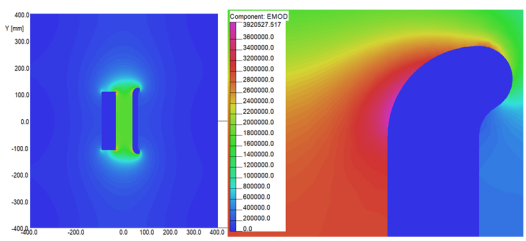

Figure 10: The 2D electric field line distribution and the electric field intensity cloud diagram of the electrode.

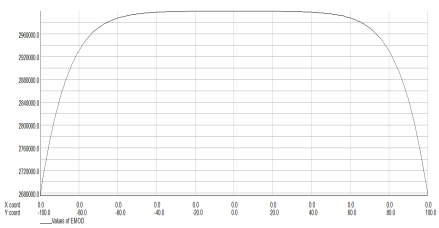

Figure 11: The vertical electric field distribution.

In the 3D simulation, the entry gap of the field-free zone is 50 mm, and the exit gap is 140 mm. The simulation result shows that the maximum field strength at the electrode is 3.77 MV, corresponding to β = 1.26. The 3D structure, the electric field line distribution diagram of the center section of the magnet, the electric field intensity cloud diagram, and the beam trajectory electric field distribution diagram are shown in Figs. 12, 13, and 14, respectively.

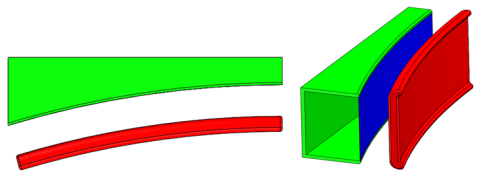

Figure 12: The 3D structure.

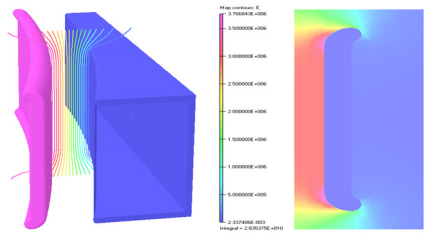

Figure 13: The electric field line distribution diagram of the center section of the magnet, the electric field intensity cloud diagram.

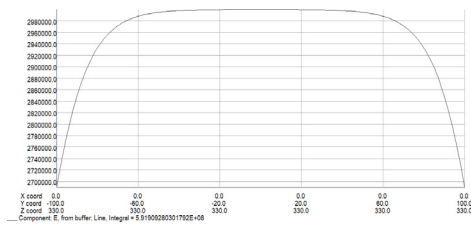

Figure 14: The beam trajectory electric field distribution diagram.

SUMMARY

The baseline scheme and the baby scheme are introduced and the physical requirements are summarized. The design of electrode is introduced. 2D and 3D simulations are carried out, and ESD with electric field concentration factor < 2 are designed. The voltage of ESD for the baseline scheme is up to 400 kV, which will bring challenges to the design and operation. The preliminary physical design has been completed. The difficulty lies in the mechanical design (high vacuum and high voltage), and further refinement and advancement are needed.

REFERENCES

[1] J. Zhang *et al.*, "Design and Realization of SFC Electrostatic Deflector Motion Control System", *Nuclear Physics Review,* vol. 33, pp. 41-44, 2016. doi:10.11804/NuclPhysRev.33.01.041

[2] X. Li *et al.*, "Design of HITFL injection and extraction high-voltage electrostatic deflector", *High Power Laser and Particle Beams*, vol. 24, pp. 2877-2879, 2012. doi:10.3788/HPLPB20122412.2877